Hindawi
Mobile Information Systems
Volume 2022, Article ID 8374901, 11 pages
https://doi.org/10.1155/2022/8374901

Research Article

Application of GPS Measurement Technology and Computer Technology in Visual Construction Simulation of Construction Engineering

Xiaowen Hu

Nantong Institute of Technology, Nantong 226002, Jiangsu, China

Correspondence should be addressed to Xiaowen Hu; 164904118@stu.cuz.edu.cn

Received 11 May 2022; Revised 23 June 2022; Accepted 29 June 2022; Published 12 August 2022

Academic Editor: Jiguo Yu

The traditional construction engineering survey has many construction problems, but also may produce large error, leading to the measurement results that cannot meet the actual requirements of the project. In this paper, a new measurement technology is proposed from the aspects of determining the angle and distance of GPS laser scanning, stitching and registration of surveying and mapping data, and GPS measurement of building engineering structures. The test results show that the measurement coincidence rate decreases with the increase of construction time. We can also obviously find the changes of visibility of different frequency points in middle and high frequency bands. The visibility of middle and high frequency band is less sensitive to construction than that of low frequency band. This method has high accuracy and can provide high accuracy for future construction and data storage. Throughout the current situation of the whole construction industry, people need to find a scientific, feasible, and efficient way to solve the problem of low efficiency and serious waste of resources. With the development of GPS measurement technology and computer technology, information technology has been deeply into various industries, such as manufacturing industry, aerospace industry, etc., through electronic information means to optimize the production technology and process, so that the production efficiency and quality have been significantly improved. Similarly, we can apply GPS measurement and computer technology to the construction industry, achieve scientific construction project management, standardize engineering technology standards, and finally achieve the ideal effect.

1. Introduction

The integration of GPS measurement technology and computer technology, the ongoing construction site measurement, and analysis of the measurement results are done in order to achieve the monitoring of engineering quality [1, 2]. The measurement work is the true reflection of the construction progress and quality and is an important technical measure for the construction unit to implement law enforcement supervision. If the measurement data is wrong, it will not only affect the follow-up quality of the project, but also reduce the expected benefits of the project [3, 4].

There are many factors that affect the production efficiency of construction industry, one of which is the unsmooth information exchange among the participants. Engineering construction is a very complex activity, involving construction units, survey units, design units, supervision units, construction units, and other departments, and with the development of the construction industry and the continuous improvement of people's living standards, The Times put forward new requirements for the construction scale, construction function, construction quality, and other aspects, and the complexity of construction, quality requirements, and the difficulty of engineering information management soared year by year. In the design stage, due to the different division of labor among different majors, it is inevitable that there will be collisions between design drawings during work, resulting in a series of design changes, bringing huge workload, thus affecting the progress of the project to a large extent. In the process of construction, the reasonable allocation of space will also directly affect the

smooth progress of construction. Due to the complexity of information of construction engineering, the phenomenon of working face conflict between different types of work sometimes occurs in the same working space, which not only has a great impact on the production efficiency, but also makes it difficult to ensure the construction quality of the structure. After the completion of the building delivery, in order to solve the problem of aging during the use of the building and meet the requirements of disaster prevention and mitigation, it is necessary to carry out effective maintenance and management, and these works need to use a large number of the original designs of the building, construction data, and drawings. There has been a lack of scientific management tools for this vital part of our lives. Due to the lack of the original design and construction data of the building, the actual maintenance scheme decisions are mostly determined according to the experience of the maintenance personnel and the capital situation of the owner, resulting in difficulties in the maintenance work.

The introduction of GPS measurement technology can not only effectively solve the problems faced by the construction industry at present, but also help the construction project to achieve information management. At the same time, it integrates all geometric characteristics, functional requirements, component performance information, construction progress, construction process control information, and other information of a construction project in the whole life cycle into a model, providing comprehensive information support for the decision-making of each stage of the whole life cycle of the construction project. And with the construction of the information model to continue to improve, it is of great significance to the improvement of project quality, the guarantee of progress, and the control of cost. In this paper, combined with the actual engineering cases, the application of GPS measurement and computer technology in the construction of construction projects is deeply analyzed.

2. Experimental Platform Construction

2.1. Preparation of Building Material Samples. In the process of GPS measurement of construction material samples, the measurement coincidence rate test was carried out, and the measurement coincidence rate of construction material samples with construction time of 0 h, 72 h, 144 h, 288 h, 576 h, 864 h, and 1152 h was measured at different measurement angles of 105°, 120°, 135°, and 150°. The construction status of building materials can be divided into three stages by using the retention rate of measuring compliance rate [5, 6].

By calculating and testing the measurement parameters of the sample building materials, it can be found that the measurement system can increase the sinusoidal voltage of a certain frequency on the sample, and the accurate measurement of the current and voltage in the sample can be calculated by using Ohm's law:

$$Z(\omega) = \frac{U(\omega)}{I(\omega)}. \tag{1}$$

Through modeling the selected building materials, the author found that impedance Z can be directly expressed by the model, and it is a measurement model commonly used for analysis [7–9]. The impedance of the model is a composite measurement, and the corresponding imaginary part represents the electric loss. The composite measurement model is shown as follows:

$$\begin{aligned} Z(\omega) &= \frac{1}{j\omega C(\omega)}, \\ C(\omega) &= C'(\omega) - jC''(\omega), \\ C'(\omega) &= \mathrm{Re}\left\{\frac{1}{j\omega Z(\omega)}\right\}, \\ C'(\omega) &= \mathrm{Re}\left\{\frac{1}{j\omega Z(\omega)}\right\}. \end{aligned} \tag{2}$$

According to the actual sample model, the same transformation calculation can be carried out for different parameters, such as visual constant and loss factor. In addition, different information of samples can be obtained by changing the SVM processing rate and voltage size to carry out more accurate profile of multiple parameters [10–12].

2.2. Initialization Parameter Test. In the experiment, the measurement angle should be set within a certain working range, such as 105°, 15°, 125°, etc., and further adopt the international standard sampling period for measurement and select the corresponding construction time of 144 h, 288 h, and 864 h. Five samples were used for accelerated GPS measurements at each measurement angle. Each sample was tested three times during the sampling time and the average of the results was taken [13].

The initial parameters of GPS measurement technology include the structure parameters and performance parameters of the sample. Among them, the measurement of different structural parameters is also to correct the structural error of construction and adjust the data error after construction and determine the datum point of the corresponding performance measurement [14–16].

3. Test and Result Analysis

3.1. Visual Constants. In this experiment, construction engineering tests are carried out on building material samples at 105°, 120°, 135°, and 150° measurement angles, and the corresponding tests are carried out on building material samples by multidimensional frequency sweep method. Here, a group of test data under different measurement angles are analyzed. The measured curves of the real and imaginary parts of the visual constant obtained at different construction times are shown in Figures 1–2 [17–19].

As can be seen from Figures 1–2, under the GPS measurement angle of 105°, the test curve features of the visible constant real part and imaginary part of the building material sample are as follows:

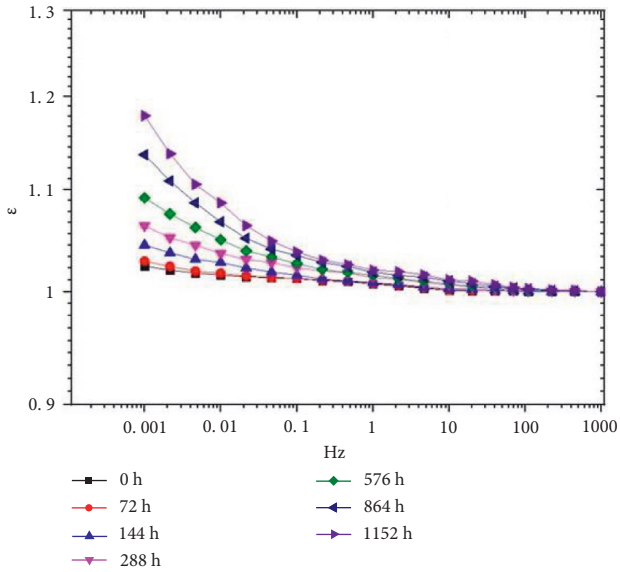

Figure 1: Real part test curve of computer simulation under 105° GPS measurement.

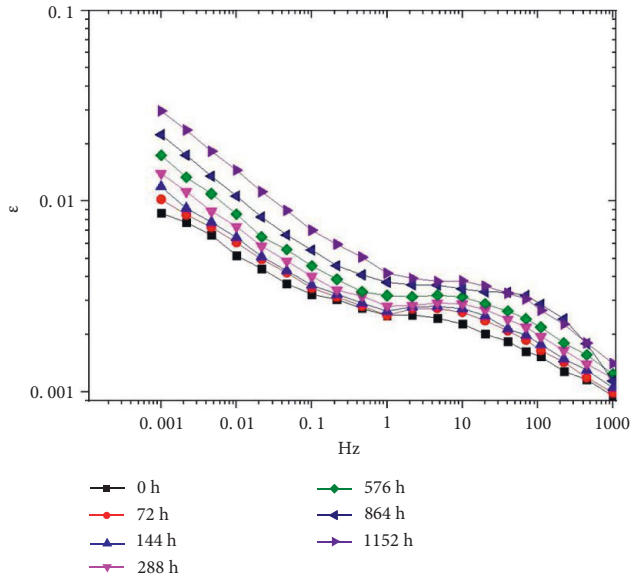

Figure 2: Virtual part test curve of computer simulation under GPS measurement at 105°.

(1) Visual constant real part curve characteristics of building material samples: from the whole test frequency band (10^{-3} Hz~10^{3} Hz), under the same construction time, the real part of visual constant shows a rising trend with the decrease of test frequency. Under the same construction time, the size of the real part of the visual constant in the high frequency band of the test curve almost remains unchanged. From the middle frequency band of the test curve, it gradually becomes larger with the decrease of frequency [20]. The dispersion is the highest in the low frequency band, and the test value of the real part of the visual constant changes more with the longer construction time. At the same test frequency, especially in the middle and low frequency segment, the test value of the real part of the visual constant increases with the construction time, and the longer the construction time, the greater the increase amplitude [21–23].

(2) Visual constant imaginary part curve characteristics of building material samples: from the whole test frequency band (10^{-3} Hz~10^{3} Hz), under the same construction time, the imaginary part of the visual constant shows a rising trend with the decrease of test frequency. Under the same construction time, with the decrease of frequency, the growth rate of visual constant imaginary part changes from large to small and becomes large again. In high frequency and low frequency band, the growth rate of visual constant imaginary part is the fastest. At the same test frequency, the longer the construction time, the greater the amplitude of the curve, and the higher the dispersion in low frequency band [24].

As can be seen from Figures 3-4, under the GPS measurement angle of 120°, the change trend of the test curve of visual constant real part and imaginary part of the construction material sample is similar to that of the 105° construction sample. With the decrease of frequency, the real and imaginary parts of visual constants show an upward trend. Similarly, in the low frequency band, the test curves of the real and imaginary parts are scattered, while in the high frequency band, the test curves are concentrated, and the curve variation rule is roughly similar to that of the 105° construction sample. In addition, compared with the 115° construction sample in the sample, the construction sample of 125° will increase with the increase of construction time. By comparing the treatment of 125° and 72 hours, it can be found that the value of the imaginary part is larger than that of the 105° construction sample [25, 26].

The real part and imaginary part of the visual constant can be calculated from 135° to 150°, and the actual change of the curve can be combined for calculation. And because the test frequency band of the real part of the visual constant can rise gradually with the decrease of the test frequency, the test curve of different construction time at the same measurement angle is 103°. With the increase of construction time, the imaginary part of the visual constant gradually increases with the decrease of frequency. The higher the measurement angle is, the greater the dispersion degree of the curve at the low frequency band is, and the curve tends to move to the high frequency [27].

Compare 120° and 150° after 1152 h 10–3 At Hz, the dispersion of curves at high frequency band also increases with the increase of measuring angle. All of these indicate that the curves of the real and imaginary parts of the visual constants are changed under the influence of the construction of building materials.

3.2. Test Platform for Measuring Compliance Rate

3.2.1. Sample Preparation. The experimental GPS used in the GPS measurement experiment was used to determine the

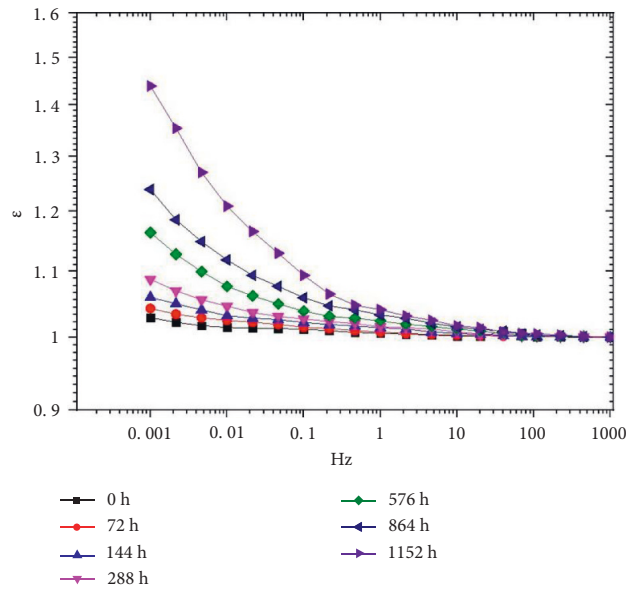

Figure 3: Real part test curve of computer simulation under 120° GPS measurement.

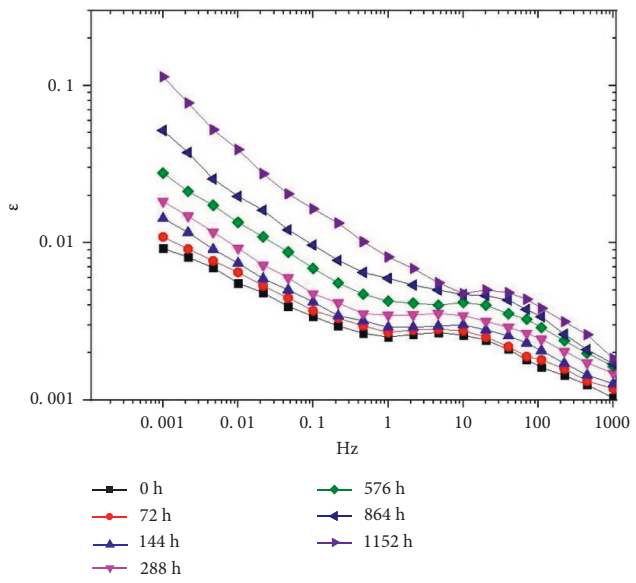

Figure 4: Virtual part test curve of computer simulation under GPS measurement at 120°.

layer material of the 10 KV construction cut-off power construction material of the distribution network. The overall process of this experiment was strictly in accordance with the relevant provisions of GB/T 2951. Firstly, the layer of the sample was cut off the ridge, and the corresponding size of the standard sample was made. And the prepared sample of building material layer is processed, and the dumbbell type sample as shown in Figure 5 below is produced by JCP-25 punching machine.

The size and shape of the experimental sample are closely related to the experimental results. Therefore, it is necessary

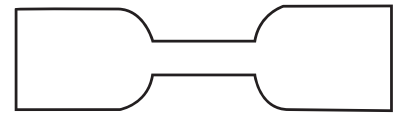

Figure 5: Shape of building materials dumbbell sample.

to use vernier calipers for accurate measurement of dumbbell head and middle stretch parts. In order to make the box angle normal and uniform it is necessary to make the air flow in the right direction. Install the air guide strip on the inner panel of the rear door and the inner front wall and side wall. The air guide section is usually rectangular. It also protects the wall from colliding with cargo. It can also be installed on the platform shelf to ensure being antislip, dry, and clean during use.

3.2.2. Test Procedure of Initial Value. The test should be carried out according to the relevant provisions of IEC60216-1:2013; first of all, the corresponding acceleration and GPS measurement test should be carried out, and further dumbbell test samples are stored in the construction of the lowest angle after 48 hours, removed, and placed in room temperature, avoiding direct sunlight. As shown in Figure 6 below, the experimental sample nos. 1–3 are relatively qualified data, while the experimental data no. 4 is invalid.

The test steps are as follows:

(1) The first pen is on the dumbbell specifications of the corresponding line marking and processing, to ensure the accurate and clear processing of the line and at the same time prevent the construction of the marking line mark volatile.

(2) In the process of testing, only vertical stretching can be felt, while the experimental sample is vertically fixed on the two experimental molds, to ensure that the marking line of the experimental sample is aligned with the edge of the mold.

(3) Set the tensile speed of the tension machine at 50 mm/min on the setting interface of the instrument.

(4) Adjust the distance between the fixture so that the instrument shows the initial stress of the fixture is 0, and then start the instrument for stretching, and then after the dumbbell sample fracture, the computer can automatically calculate the maximum tensile force and tensile length at this time and automatically calculate the original length ratio between the corresponding length and the experimental sample.

3.3. Test Results and Analysis. In this experiment, five dumbbell samples were selected for the initial measurement coincidence rate test. Three dumbbell samples with GPS measurement were taken out at each sampling time and then tested according to the above steps after they were placed at

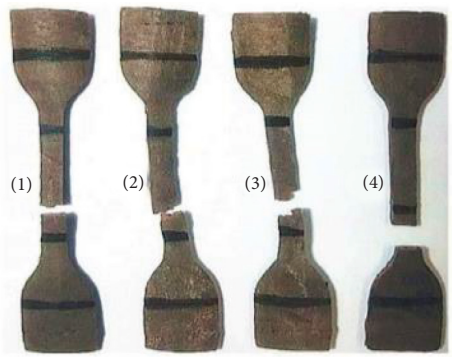

Figure 6: Test data judgment criteria.

room temperature for 16 hours. The average value of the test results was taken. The test results are as Tables 1–5.

From the above experimental test results, it can be clearly found that the coincidence rate of measurement will decrease with the increase of construction time, and its rate of decline is affected by the measurement angle. The higher the angle, the greater the corresponding reduction, which indicates that the corresponding building material measurement technology can be used more quickly. At the same measurement angle, the reduction of the measurement coincidence rate in the initial construction period is not obvious. In the later period, the construction rate is gradually accelerated, and the corresponding growth range has also been greatly increased.

Construction stage classification of building materials: In front of the building materials construction status classification, first of all, according to the experiment of measuring coincidence rate and the construction status of building materials division, GB/T 11026.2 2003 shows that coincidence rate can be used as a measurement technology in the construction state standards; on this basis, according to the measurement of coincidence rate of retention, construction stage can be classified. The measurement compliance rate retention rate is calculated as follows:

$$\mathrm{EAB}\% = \frac{\mathrm{EAB}'}{\mathrm{EAB}_0}. \tag{3}$$

where: EAB% is the retention rate of the measurement compliance rate; EAB' is the initial measurement compliance rate; EAB0 is the sample measurement compliance rate after construction.

Three dumbbell samples for accelerated GPS measurement were taken out at each sampling time and tested after their angles dropped to room temperature. The average value was taken, and the test results were shown in Tables 6-7. According to the retention rate data of measurement compliance rate in Tables 6-7, the construction state of construction material samples under different measurement angles and different construction times is classified. The sample with EAB% within the range of 100% to 75% is called condition "1", indicating that the construction material is in good condition. Samples with EAB% in the range of 75% to

Table 1: Initial measurement compliance rate test.

The sample number	1	2	3	4	5	The average
The EAB (%)	502.31	511.74	509.83	505.18	512.52	508.31

Table 2: Measurement compliance rate test at 105° measurement angle.

Measure the angle (°)	Construction time (h)	Measurement compliance rate (%)		
105	0	508.31	508.31	508.31
	72	505.21	503.01	504.89
	144	489.81	495.64	494.21
	288	477.68	473.57	480.84
	576	439.34	434.01	441.28
	864	388.03	378.43	376.47
	1152	317.13	326.26	323.25

Table 3: Measurement compliance rate test at 120° measurement angle.

Measure the angle (°)	Construction time (h)	Measurement compliance rate (%)		
120	0	508.31	508.31	508.31
	72	487.33	479.75	482.88
	144	461.99	463.87	459.09
	288	427.9	429.53	425.51
	576	370.03	362.15	363.95
	864	299.53	307.81	309.7
	1152	255.5	263.19	261.01

Table 4: Measurement compliance rate test at 135° measurement angle.

Measure the angle (°)	Construction time (h)	Measurement compliance rate (%)		
135	0	508.31	508.31	508.31
	72	474.71	478.21	471.03
	144	436.21	436.88	443.85
	288	381.1	383.05	379.12
	576	326.74	331.81	330.5
	864	255.04	247.56	254.01
	1152	190.35	185.64	184.94

Table 5: Measurement compliance rate test at 150° measurement angle.

Measure the angle (°)	Construction time (h)	Measurement compliance rate (%)		
150	0	508.31	508.31	508.31
	72	479.23	477.56	473.17
	144	445.28	441.25	448.83
	288	355.91	354.51	348.53
	576	245.09	243.19	247.47
	864	148.81	142.33	142.6
	1152	70.43	62.58	63.07

Table 6: Test values of measurement compliance rate of construction samples.

Angle (°)	Construction time (h)	Measurement compliance rate (%)	Measurement compliance rate retention rate (%)	Condition number	Angle (°)	Construction time (h)	Measurement compliance rate (%)	Measurement compliance rate retention rate (%)	Condition number
105	0	508.31	100	1	120	0	508.31	100	1
105	72	504.37	99.22	1	120	72	483.32	95.08	1
105	144	493.22	97.03	1	120	144	461.65	90.82	1
105	288	477.36	93.91	1	120	288	427.65	84.13	1
105	576	438.21	86.2	1	120	576	365.38	71.88	2
105	864	380.98	74.95	2	120	864	305.68	60.13	2
105	1152	322.21	63.38	2	120	1152	259.9	51.13	2
135	0	508.31	100	1	150	0	508.31	100	1
135	72	474.65	93.37	1	150	72	476.65	93.77	1
135	144	438.98	86.36	1	150	144	445.12	87.56	1
135	288	381.09	74.97	2	150	288	352.98	69.44	2
135	576	329.68	64.85	2	150	576	245.25	48.24	3
135	864	252.2	49.61	3	150	864	144.58	28.44	3
135	1152	186.98	36.78	3	150	1152	65.36	12.85	3

Table 7: 105° measurement angle.

Measure the angle (°)	Construction time (h)	Tan delta integral of low frequency band	Integral value of tanδ in middle frequency band	High frequency tanδ integral value	Condition number
105	0	0.00286	0.1968	1.01526	1
105	72	0.00297	0.22323	1.06998	1
105	144	0.00309	0.23419	1.14619	1
105	288	0.00332	0.25587	1.25936	1
105	576	0.00367	0.28106	1.37506	1
105	864	0.0044	0.35064	1.57824	2
105	1152	0.00543	0.34862	1.62035	2

50% are denoted as condition "2", indicating that there is a certain risk of construction materials. The sample with EAB % below 50% is status "3", indicating that the construction material needs repair or replacement.

3.3.1. Feature Extraction. GPS simulation in frequency domain can reveal the properties of building materials to a certain extent. It is related to the measurement performance of materials and is not affected by the size of building materials. The construction material loss technology is nondestructive and has a significant advantage in evaluating the construction condition of GPS measurement. As can be seen from the above analysis of GPS measurement experimental data, the simulated tangent value of GPS measurement technology is directly related to the frequency. In the continuous construction of GPS measurement technology, its measurement spectrum in frequency domain is also changing. Therefore, this paper extracted the integral value of GPS simulated tangent value in different frequency bands, slope, and curvature of fitting curve as characteristic values and made the sample set of subsequent support vector machines.

3.3.2. Integral Value of GPS Simulated Tangent Value. The experimental data measured by GPS are analyzed above, and the construction engineering characteristics of building materials under different measurement angles and different construction duration have been obtained. It can be concluded that there is a close relationship between GPS simulated tangent value and construction of building materials. The integral value of GPS simulated tangent value is selected as the characteristic value to evaluate the construction stage of building materials and observe its correlation with construction site of building materials. According to the analysis of the ground experiment results, it can be concluded that the sensitivity of GPS simulated tangent values in different frequency bands to construction is different, and the sensitivity of low frequency visibility to construction is much higher than that of medium-high frequency band. Therefore, the frequency stage is divided into three stages according to the different sensitivity of GPS simulated tangent values of building materials to construction. The integral values of GPS analog tangent values in three frequency band stages are obtained. Tables 7–10 show the integral values of GPS simulated tangent values of construction material samples with different angles and different construction time in low frequency band (0.001 Hz–1 Hz), middle frequency band (1 Hz–100 Hz), and high frequency band (100 Hz–1000 Hz).

3.3.3. Slope and Curvature of Fitting Curve. In the previous section, the integral value of GPS simulated tangent value at different frequency stages has been obtained. The scatter plots of different stages are drawn with construction

Table 8: 120° measurement angle.

Measure the angle (°)	Construction time (h)	Tan delta integral of low frequency band	Integral value of tan in middle frequency band	High frequency tan integral value	Condition number
120	0	0.00285	0.21935	1.10214	1
120	72	0.00314	0.23303	1.20677	1
120	144	0.00338	0.26862	1.31481	1
120	288	0.00391	0.30945	1.55828	1
120	576	0.00518	0.37621	1.78686	2
120	864	0.00713	0.44163	1.91156	2
120	1152	0.01117	0.4962	2.26033	2

Table 9: 135° measurement angle.

Measure the angle (°)	Construction time (h)	Tan delta integral of low frequency band	Integral value of tan in middle frequency band	High frequency tan integral value	Condition number
135	0	0.00262	0.20995	1.29317	1
135	72	0.00273	0.2265	1.33775	1
135	144	0.00349	0.25383	1.36954	1
135	288	0.00441	0.32349	1.62567	2
135	576	0.00597	0.3859	1.87025	2
135	864	0.00974	0.49517	2.50187	3
135	1152	0.01953	0.69442	3.02835	3

Table 10: 150° measurement angle.

Measure the angle (°)	Construction time (h)	Tan delta integral of low frequency band	Integral value of tan in middle frequency band	High frequency tan integral value	Condition number
150	0	0.00263	0.21159	1.13373	1
150	72	0.00282	0.22078	1.30275	1
150	144	0.00407	0.25223	1.43401	1
150	288	0.00589	0.39023	1.98245	2
150	576	0.01121	0.45236	2.15705	3
150	864	0.02313	0.56437	2.7236	3
150	1152	0.07523	0.80393	3.46921	3

Table 11: Integral fitting formula of low frequency GPS simulated tangent values at different measurement angles.

Measuring angle	Integral fitting formula of low frequency GPS simulated tangent value	R^2
105°	$\int \tan\ \text{delta} = 7.14302e-4 * \exp\ (t/764.38139) + 0.0022$	0.9964
120°	$\int \tan\ \text{delta} = 0.00108 * \exp\ (t/537.66027) + 0.00192$	0.99748
135°	$\int \tan\ \text{delta} = 7.52137e-4 * \exp\ (t/367.66815) + 0.00219$	0.99487
150°	$\int \tan\ \text{delta} = 5.45319e-4 * \exp\ (t/235.90665) + 0.00304$	0.99718

duration as abscissa and integral value of GPS simulated tangent value as ordinate. It can be obtained from the scatter plot analysis: At the same angle, the integral value of GPS simulated tangent value in the same frequency band is positively correlated with the construction time, and there is a certain functional relationship between the integral value and the construction time. By observing the dispersion of points and fitting with different functions, it is found that the fitting effect of exponential function is better. Therefore, according to the integral values of GPS simulated tangent values of each frequency band calculated above, the integral values of GPS simulated tangent values of different frequency bands are fitted by exponential function. Table 11 below is the fitting curve and its fitting formula of integral values of GPS simulated tangent values at different frequencies and angles.

Through the exponential fitting curves and fitting formulas above in different frequency bands, the mathematical relationship between the integral value of THE GPS simulated tangent value and the construction time was obtained. In order to extract more variation characteristics of the fitting curve, the slope and curvature of the tangent line at each point of the fitting curve in three frequency bands were selected as characteristic parameters. According to the fitting formula, the slope and curvature of the integral fitting curve of GPS simulated tangent value at different points are obtained by using the function derivation rule and curvature calculation formula.

Table 12: 105° measurement angle.

Construction time (h)		0	72	144	288	576	864	1152
Tan delta integral value	Low	0.00286	0.00297	0.00309	0.00332	0.00367	0.0044	0.00543
	In the middle	0.1968	0.22323	0.23419	0.25587	0.28106	0.35064	0.34862
	High	1.01526	1.06998	1.14619	1.25936	1.37506	1.57824	1.62035
The tangent slope	Low	$9.38725934e-7$	$1.02683381e-6$	$1.12788469e-6$	$1.36182517e-6$	$1.98533898e-6$	$2.8943296e-6$	$4.21473151e-6$
	In the middle	$2.09634e-4$	$1.9725e-4$	$1.85553e-4$	$1.64117e-4$	$1.28389e-4$	$1.00439e-4$	$7.88247e-5$
	High	$9.19788e-4$	$8.54067e-4$	$4.00839e-7$	$6.8274e-4$	$5.0633e-4$	$1.35515e-7$	$1.9615e-8$
The curvature	Low	$3.58913e-10$	$1.70046e-9$	$3.7425e-9$	$2.82129e-9$	$3.24664e-9$	$5.9944e-9$	$2.75488e-9$
	In the middle	$8.92667e-8$	$2.1276e-7$	$7.92805e-4$	$2.21389e-7$	$1.36744e-7$	$3.75501e-4$	$2.79563e-4$
	High	$4.76817e-7$	$1.12163e-6$	$2.08514e-6$	$1.12132e-6$	$6.56595e-7$	$6.16864e-7$	$8.47252e-8$
Condition serial number		1	1	1	1	1	2	2

Table 13: 120° measurement angle.

Construction time (h)		0	72	144	288	576	864	1152
Tan delta integral value	Low	0.00285	0.00314	0.00338	0.00391	0.00518	0.00713	0.01117
	In the middle	0.21935	0.23303	0.26862	0.30945	0.37621	0.44163	0.4962
	High	1.10214	1.20677	1.31481	1.55828	1.78686	1.91156	2.26033
The tangent slope	Low	$2.01989e-6$	$2.29465e-6$	$2.62223e-6$	$3.42803e-6$	$5.85859e-6$	$1.00125e-5$	$1.70841e-5$
	In the middle	$3.31356e-4$	$3.17678e-4$	$3.04523e-4$	$2.79729e-4$	$2.36033e-4$	$1.99163e-4$	$1.68424e-4$
	High	0.0014	0.00131	0.00126	0.00113	$9.09478e-4$	$7.31777e-4$	$5.90464e-4$
The curvature	Low	$1.09887e-9$	$5.40229e-9$	$1.23713e-8$	$1.00972e-8$	$1.36206e-8$	$2.94791e-8$	$1.58704e-8$
	In the middle	$9.76198e-8$	$2.3705e-7$	$4.55121e-7$	$2.61057e-7$	$1.73915e-7$	$1.85894e-7$	$2.89827e-8$
	High	$5.29368e-7$	$1.19535e-6$	$2.41042e-6$	$1.35015e-6$	$8.57715e-7$	$8.74237e-7$	$1.30084e-7$
Condition serial number		1	1	1	1	2	2	2

Table 14: 135° measurement angle.

Construction time (h)		0	72	144	288	576	864	1152
Tan delta integral value	Low	0.00262	0.00273	0.00349	0.00441	0.00597	0.00974	0.01953
	In the middle	0.20995	0.2265	0.25383	0.32349	0.3859	0.49517	0.69442
	High	1.29317	1.33775	1.36954	1.62567	1.87025	2.50187	3.02835
The tangent slope	Low	$2.06507e-6$	$2.48846e-6$	$3.02469e-6$	$4.47569e-6$	$9.79987e-6$	$2.14575e-5$	$4.68725e-5$
	In the middle	$2.11826e-4$	$2.27312e-4$	$2.44727e-4$	$2.8383e-4$	$3.81778e-4$	$5.13528e-4$	$6.90129e-4$
	High	$9.20683e-4$	$9.74877e-4$	0.00103	0.00117	0.00148	0.00189	0.0024
The curvature	Low	$1.64505e-9$	$8.56711e-9$	$2.08712e-8$	$1.92802e-8$	$3.33177e-8$	$9.23766e-8$	$6.3643e-8$
	In the middle	$6.36674e-8$	$2.96049e-7$	$6.386e-7$	$4.62428e-7$	$4.91003e-7$	$8.36467e-7$	$3.54818e-7$
	High	$2.24259e-7$	$1.02926e-6$	$2.18929e-6$	$1.54147e-6$	$1.54741e-6$	$2.4923e-6$	$9.9975e-7$
Condition serial number		1	1	1	2	2	3	3

The tangent slope of the fitting curve of integral value represented at construction time t is defined, and the calculation formula is shown in formula (4): $y'(t)\tan\delta y = \int \tan\delta$

$$y'(t) = \frac{dy}{dt}. \tag{4}$$

Define the curvature of the fitting curve represented by k at construction time t. $\tan\delta y = \int \tan\delta$.

The curvature calculation formula is shown in the following equation:

$$k = \left| \frac{y''}{\left(1 + y'^2\right)^{3/2}} \right|. \tag{5}$$

Some characteristic parameters obtained through the above analysis are shown in Tables 12–15.

Tables 4–8 to 9–15 above only show one of the five sets of data of GPS measurement experiment under each GPS measurement angle and construction duration. A total of 140 sets of data have been extracted in this paper, and 9-dimensional characteristic parameters constitute the sample set of support vector machine.

Table 15: 150° measurement angle.

Construction time (h)		0	72	144	288	576	864	1152
Tan delta integral value	Low	0.00263	0.00282	0.00407	0.00589	0.01121	0.02313	0.07523
	In the middle	0.21159	0.22078	0.25223	0.39023	0.45236	0.56437	0.80393
	High	1.13373	1.30275	1.43401	1.98245	2.15705	2.7236	3.46921
The tangent slope	Low	$2.34582e-6$	$3.13709e-6$	$4.25218e-6$	$7.83145e-6$	$2.65646e-5$	$9.01084e-5$	$3.04533e-4$
	In the middle	$3.4132e-4$	$3.55922e-4$	$3.71869e-4$	$4.06081e-4$	$4.84237e-4$	$5.77435e-4$	$6.88207e-4$
	High	0.00174	0.00176	0.00178	0.00182	0.00191	0.002	0.00209
The curvature	Low	$2.91923e-9$	$1.68317e-8$	$4.57423e-8$	$5.25878e-8$	$1.40759e-7$	$6.0449e-7$	$6.43878e-7$
	In the middle	$6.08714e-8$	$2.7523e-7$	$5.76099e-7$	$3.92801e-7$	$3.69764e-7$	$5.58474e-7$	$2.10133e-7$
	High	$8.32023e-8$	$3.54887e-7$	$7.19075e-7$	$4.59409e-7$	$3.79705e-7$	$5.03522e-7$	$1.2481e-7$
Condition serial number		1	1	1	2	3	3	3

Table 16: Characteristic values and contribution rate.

The serial number	The eigenvalue	The contribution rate of *Kr* %	Cumulative contribution *Kt* %
1	5.43309709762376	60.36775	60.36775
2	1.95106975984693	21.67855	82.0463
3	0.797370017523492	8.859667	90.90597
4	0.488039553923280	5.422662	96.32863
5	0.243969785042391	2.710775	99.0394
6	0.0739347774239264	0.821498	99.8609
7	0.00747370404445418	0.083041	99.94394
8	0.00436948766222832	0.04855	99.99249
9	0.000675816909545564	0.007509	100

As the parameters in the input sample set contain physical quantities of different properties, the values of all kinds of sample parameters differ greatly. In order to eliminate the dimensionality between parameters and make them comparable, it is necessary to normalize all kinds of sample parameters of the input data according to formula (6).

$$y_i = \frac{x_i - x_{\min}}{x\min_{\max}}. \tag{6}$$

3.3.4. Dimension Reduction of Feature Information Based on PCA Method. It can be clearly found from the foregoing that PCA based method can effectively extract the nine-dimensional features of pattern recognition, and there is redundant information between different feature values. If the high-latitude eigenvalues are directly connected to the classifier for training and classification, it is easy to bring huge burden to the classifier, and it is difficult for the classifier to classify, and serious misclassification may occur again. The following corresponding work needs to extract the corresponding optimal feature quantity from the features of high latitude and extract the corresponding redundant features and carry out multiple optimizations on the feature space, which can not only optimize the original feature value of high dimension, but also improve the accuracy and speed of recognition. From the analysis of main components, it can be found that fewer parts should be extracted for corresponding processing for the classification of feature information mentioned in above contents.

Table 17: Comparison of recognition accuracy before and after dimensionality reduction.

	Recognition accuracy (%)
Dimension reduction before	90.91
After the dimension reduction	98.18

The characteristic parameters extracted were analyzed by principal component analysis, and a 9-dimensional parameter matrix was extracted. Firstly, equations (4)-(4) are used to construct the covariance matrix. The eigenvalues and corresponding contribution rates of covariance matrix C are listed in Table 16. Table 17 shows the change of single contribution rate with principal component, according to which correlation analysis of dimension reduction effect can be conducted.

It can be further analyzed from the table above that the contribution rate of the first five principal components should be higher than 99%, and from the sixth component, it can be found that the corresponding change degree is relatively low. Their contribution rates add up to less than one percent.

3.3.5. Support Vector Machines. Based on the training sample *D*, the linear classifier can find a hyperplane in two-dimensional space to separate the two kinds of samples. Of course, there are many such hyperplanes, but there is only one partition hyperplane that satisfies the maximum linear interval that $w \cdot \text{bob} = 0$ in Figure 7 is the ideal segmented hyperplane, because the partition hyperplane has the best "tolerance" to the local disturbance of the training sample and the strongest generalization ability.

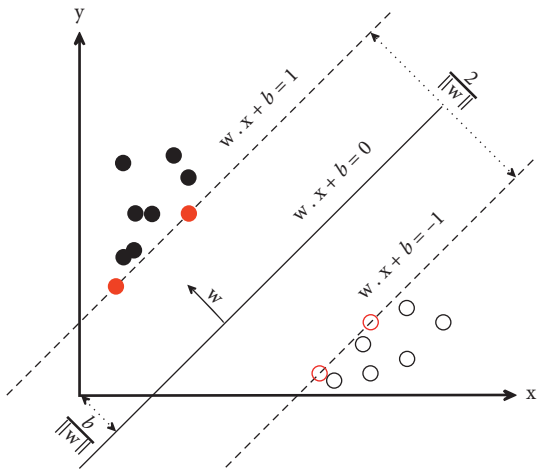

Figure 7: Optimal classification surface.

Table 18: Identification results of construction stage.

The construction phase	Training/test samples	Recognition accuracy (%)
Construction stage condition "1"	40/35	97.14
Condition of construction phase "2"	30/10	100
Condition of construction stage "3"	15/10	100

As shown in Figure 7, for a given sample set, N is the two question labels and M is the number of samples. −1 is a negative example, and 1 is a positive example: $S = (x_1, y_1), (x_2, y_2), \ldots, (x_m, y_m) x_i \in R_D y_i \in \{-1, +1\} y_i$

$$w^T x + b = 0. \tag{7}$$

Among them:

$x = x_1, x_2, \ldots, a_m$ is the input data and dimension is M.

$w = w_1, w_2, \ldots, w_d$ is the normal vector, which determines the direction of the hyperplane.

$$\gamma = \frac{|w^T x + b|}{w}. \tag{8}$$

3.3.6. Analysis of Identification Results. By analyzing the experimental data, fitting the tangent of GPS simulation under different frequency band is integral value and construction of long fitted curve to extract the tangent GPS simulation under different frequency band is integral value; the different construction time tangent slope and curvature characteristic value obtained a total of 140 sets of data to do sample set for training and prediction of support vector machine (SVM). Eighty-five groups of samples were used for training SVM classifier, and 55 groups were used for testing. The recognition results are shown in Table 18.

It can be seen from the identification results that only one of the 55 test samples with the condition of "1" in the construction stage is wrong, and the rest of the test samples are correctly predicted, with the overall identification accuracy as high as 98.18%.

4. Conclusion

At a certain measurement angle, from the overall test frequency band (10^{-3} Hz~10^3 Hz), the simulated tangent value of GPS increases gradually with the decrease of test frequency. In the middle and high frequency band (1 Hz~103 Hz), the curve of GPS simulated tangent value is more concentrated and overlapped, and the value of GPS simulated tangent increases with the increase of construction time. At the lower frequencies (10^{-3} Hz~1 Hz), the tangent value of GPS simulation changes more obviously with the increase of construction time, and the amplitude is larger. Low frequency band is more sensitive to construction time and angle. The test results show that the measurement coincidence rate decreases with the increase of construction time. We can also obviously find the changes of visibility of different frequency points in middle and high frequency bands. The visibility of middle and high frequency band is less sensitive to construction than that of low frequency band. However, with the extension of construction time, the visibility gradually presents an increasing trend, and the impact of construction on the building material samples of GPS is positively correlated.

Data Availability

The data used to support the findings of this study are available from the author upon request.

Conflicts of Interest

The author declares that there are no conflicts of interest.

Acknowledgments

This research study was sponsored by School-Level Project of Nantong Institute of Technology. The name of the project is training of young- and middle-aged scientific research backbone in Nantong Institute of Technology (project no. ZQNGG403).

References

[1] N. P. Rønnest, S. M. Stocks, A. Eliasson Lantz, and K. V. Gernaey, "Introducing process analytical technology (PAT) in filamentous cultivation process development: comparison of advanced online sensors for biomass measurement," *Journal of Industrial Microbiology & Biotechnology*, vol. 38, no. 10, pp. 1679–1690, 2011.

[2] P. C. Nie, D. Wu, W. C. Zhang, Y. Yang, and Y. He, "Hybrid combination of GIS, GPS, WSN and GPRS technology in modern digital agriculture application," *Advanced Materials Research*, vol. 108, pp. 1158–1163, 2010.

[3] G. M. Zhan, Z. W. Li, X. J. Liu, and K. Zhong, "Hand-held blue light 3D measurement technology and its application in hot stamping," *Advanced Materials Research*, vol. 1063, pp. 362–366, 2014.

[4] M. Z. Stalker, A. B. Kornblith, P. M. Lewis, and R. Parker, "Measurement technology applications in performance appraisal," *Jona the Journal of Nursing Administration*, vol. 16, no. 4, pp. 12–17, 1986.

[5] X. F. Liu, "Measurement technology in the application of the housing construction," *Advanced Materials Research*, vol. 971, pp. 2111–2114, 2014.

[6] X. P. Zhou, "Based on GPS RTK technology in open pit mine in the measurement of the application research," *Advanced Materials Research*, vol. 748, pp. 565–570, 2013.

[7] R. Wirahadikusumah and D. M. Abraham, "Application of dynamic programming and simulation for sewer management," *Engineering Construction and Architectural Management*, vol. 10, no. 3, pp. 193–208, 2003.

[8] T. Waroonkun and R. A. Stewart, "Modeling the international technology transfer process in construction projects: evidence from Thailand," *The Journal of Technology Transfer*, vol. 33, no. 6, pp. 667–687, 2008.

[9] K. Flaga and K. Furtak, "Application of composite structures in bridge engineering. Problems of construction process and strength analysis," *Civil and Environmental Engineering Reports*, vol. 15, no. 4, pp. 57–85, 2015.

[10] L. Dou and H. Li, "Analysis of the key and difficult points in the engineering construction technology of the steel structures of a super high-rise building," *IOP Conference Series: Materials Science and Engineering*, vol. 224, Article ID 012059, 2017.

[11] Research, "Interactive pentablet measurement of symptoms by hospice cancer patients in their homes," *Journal of Palliative Medicine*, vol. 12, no. 7, pp. 599–602, 2009.

[12] S. Kawabata, M. Niwa, and Y. Yamashita, "Recent developments in the evaluation technology of fiber and textiles: toward the engineered design of textile performance," *Journal of Applied Polymer Science*, vol. 83, no. 3, pp. 687–702, 2002.

[13] A. Nikakhtar, A. A. Hosseini, K. Y. Wong, and A. Zavichi, "Application of lean construction principles to reduce construction process waste using computer simulation: a case study," *International Journal of Services and Operations Management*, vol. 20, no. 4, p. 461, 2015.

[14] D. Gotthold, S. Govindaraju, J. Reifsnider, G. Kinsey, J. Campbell, and A. Holmes, "Molecular-beam epitaxy growth of Ga(In)NAs/GaAs heterostructures for photodiodes," *Journal of Vacuum Science & Technology B: Microelectronics and Nanometer Structures*, vol. 19, no. 4, p. 1400, 2001.

[15] S. Toogood, "Behavioural observation: technology and application in developmental disabilities," *Journal of Applied Research in Intellectual Disabilities*, vol. 15, no. 1, pp. 109-110, 2002.

[16] M. Li, W. van Keulen, E. Tijs, M. van de Ven, and A. Molenaar, "Sound absorption measurement of road surface with in situ technology," *Applied Acoustics*, vol. 88, pp. 12–21, 2015.

[17] J. Q. Liang, S. H. Zhao, J. L. Wang, and Z. G. Du, "Research and design of a fusion technology in highway engineering measurement and payment system," *Advanced Engineering Forum*, vol. 1, pp. 62–65, 2011.

[18] Y. S. Zhang, R. Y. Li, and F. Wen, "Application of GPS-RTK technology in the measurement of discontinuity traces," *Advanced Materials Research*, vol. 594, pp. 2371–2374, 2012.

[19] Y. Li and H. J. Xu, "The study and application of beating degree's soft-measurement technology based on FBP algorithm in product materials system," *Applied Mechanics and Materials*, vol. 63, pp. 295–298, 2011.

[20] Y. P. Qin, "Application of virtual reality technology in construction control and management," *Applied Mechanics and Materials*, vol. 427, pp. 2851–2854, 2013.

[21] K. Aksyonov, E. Bykov, and O. Aksyonova, "Application of multi-agent simulation for decision support in a construction corporation and its comparison with critical path method," *Applied Mechanics and Materials*, vol. 278, pp. 2244–2247, 2013.

[22] L. Li and L. X. Wang, "Application of BIM technology in green building engineering construction," *Advanced Materials Research*, vol. 860, pp. 1301–1305, 2013.

[23] H. Zhang, D. L. Xun, Z. Yang, and F. Q. Ji, "Application of new soil consolidator in road-construction engineering," *Applied Mechanics and Materials*, vol. 238, pp. 466–469, 2012.

[24] W. Y. Gong and B. Bai, "Waterproof and impermeability technology strategy of constructional engineering," *Advanced Materials Research*, vol. 557, pp. 818–821, 2012.

[25] P. A. Pebsworth, H. R. Morgan, and M. A. Huffman, "Evaluating home range techniques: use of Global Positioning System (GPS) collar data from chacma baboons," *Primates*, vol. 53, no. 4, pp. 345–355, 2012.

[26] X. F. Chen, P. Cheng, and L. Wu, "Application of value engineering in construction project management of hydraulic and hydroelectric engineering," *Advanced Materials Research*, vol. 1065, pp. 2424–2427, 2014.

[27] B. Chen, H. Ren, and L. X. Fu, "On the portal construction technology of spiral tunnel in special stratum," *Applied Mechanics and Materials*, vol. 94, pp. 1879–1884, 2011.